Terahertz current oscillations assisted by optical phonon emission in GaN n^+nn^+ diodes: Monte Carlo simulations

A. Íñiguez-de-la-Torre, J. Mateos,[a] and T. González
Departamento de Física Aplicada, Universidad de Salamanca, Plaza de la Merced s/n, 37008 Salamanca, Spain

(Received 26 November 2009; accepted 12 January 2010; published online 3 March 2010)

Under certain conditions, plasma instabilities associated with streaming motion of carriers taking place in n^+nn^+ diodes can lead to current oscillations. The origin of the phenomenon, known as optical phonon transit time resonance, is characterized by a frequency related to the transit time between consecutive optical phonon emissions by electrons along the active region of the diode. By means of Monte Carlo simulations, the possibility to obtaining current oscillations in GaN n^+nn^+ diodes is analyzed. The optimum conditions for the onset of such mechanism are investigated: applied bias, temperature, doping, and length of the active n region. Simulations show that current oscillations at frequencies in the terahertz range can be obtained at very low temperatures. Moreover, by choosing the appropriate applied voltage and length of the n region, some degree of tunability can be achieved for frequencies close to the plasma frequency of the n region of the n^+nn^+ diode. © *2010 American Institute of Physics*. [doi:10.1063/1.3309790]

I. INTRODUCTION

Terahertz radiation, whose frequency lies between the microwave and the infrared regions of the electromagnetic spectrum, is one of the most promising research areas in the past few years. The development of terahertz power sources has generated intense interest because of its applications in a wide range of fields as material characterization, microelectronics, astronomy, weapon detection, medical diagnosis, environmental control, and chemical and biological identification.[1–3] The lack of suitable technologies led to the terahertz band being called the "terahertz gap."[4]

The progress for filling the terahertz gap has came from both sides of the electromagnetic spectrum: optics and electronics. On the optics side, the quantum cascade laser is the main terahertz emitter useful to bridge the gap.[5] On the other side, into the electronics branch there are various methods that have been studied with regard to the achievement of terahertz sources.[6] Among them we would like to emphasize the promising expectatives of the so-called optical phonon transit time resonance (OPTTR), a phenomenon taking place in structures based on III-V semiconductors with high-energy optical phonons.[7–9] When operating at small bias and at sufficiently low lattice temperatures, optical phonon emission (OPE) is the dominant scattering mechanism in these semiconductors. In this situation, plasma instabilities associated with the streaming motion of carriers, characterized by a frequency related to the transit time of electrons between two consecutive emissions, can take place, giving rise to current oscillations under some specific conditions.[10–14]

Experimental evidences of this phenomenon are humps observed in the *I-V* curves of InSb,[15] GaAs,[16] InGaAs,[17] and InP[18] diodes when the applied voltage reaches the threshold for one, two, and three OPEs. As ultimate confirmation of the OPTTR, the generation of millimeter-wave radiation in InP with a frequency following the characteristic bias dependence of the process has been detected.[19]

The aim of this work is to study, by means of Monte Carlo (MC) simulations, the onset of OPTTR induced current oscillations in n^+nn^+ structures and their dependence on various magnitudes such as temperature, applied voltage, and doping and length of the n region. While the phenomenon has been previously studied in InN,[7] InP,[20,21] and GaAs n^+nn^+ structures,[22] in this paper, we will deal with the case of GaN diodes. So far, only ideal bulk material properties related to the OPPTR were studied in GaN,[23] showing that it is a promising candidate for terahertz sources due to its high value of the optical phonon energy.

The content of this paper is structured as follows. In Sec. II the OPTTR phenomenon and the conditions for obtaining oscillations are explained; Sec. III presents the simulation method and the features of the modeled structures; in Sec. IV the results obtained in bulk GaN and n^+nn^+ diodes by means of MC simulations are shown and discussed; and finally, major conclusions are presented in Sec. V.

II. OPTTR: CONCEPT AND CONDITIONS

A. Single particle

In a III-V semiconductor material at very low temperature the absorption of optical phonons is basically absent, while OPE is the dominant scattering mechanism electrons suffer. In these conditions the dynamics of an electron subjected to a constant electric field E is very simple. The carrier is ballistically accelerated by the field until reaching the energy necessary for emitting an optical phonon ($\hbar\omega_0$). Then, the OPE takes place so that the electron loses practically all its energy and stops. Next, there will be another acceleration and the consequent stop when emitting the following optical phonon. Obviously, this dynamics is repeated throughout the

[a]Electronic mail: javierm@usal.es.

whole material and gives rise to a clear modulation in the value of the velocity of every single electron. This process is spatially periodic with a characteristic length given by

$$l_0 = \frac{\hbar\omega_0}{eE}, \tag{1}$$

where e is the electron charge; and it is also periodic in time with a period, called transit time, which can be written as

$$\tau_E = \sqrt{2m_0 m^* \hbar\omega_0}/eE, \tag{2}$$

where m^* and m_0 are the effective and free electron masses, respectively.[7]

In fact, the main interest of this phenomenon is that its characteristic frequency,

$$f_E = 1/\tau_E, \tag{3}$$

lies within the terahertz range. For this reason, the exploitation of OPTTR to obtain current oscillations of such high frequency is of high interest and deserves further investigation. Moreover, if the optical phonon energy of the material is high, the phenomenon occurs more significantly because of the stronger modulation of velocity. This is the case of GaN, for which $\hbar\omega_0 = 0.091$ eV.

B. Collective phenomenon

If we now consider a real device with a large amount of electrons, the stopping processes will lead to carrier accumulations, thus giving rise to a nonuniform electric field.

Achieving oscillations in the current within a device requires that the OPTTR process takes place in a coherent (and therefore collective) way, i.e., the phonon emissions must be synchronized by means of the self-consistent electric field. This phenomenon will inevitably be influenced by the parameters characterizing the electronic plasma and the conditions for oscillations.[24]

First, carrier accumulations can reinforce the spontaneous charge oscillations taking place in the semiconductor at the plasma frequency,

$$f_p = \frac{e}{2\pi}\sqrt{\frac{N}{m^* m_0 \varepsilon_0 \varepsilon_r}}, \tag{4}$$

where N is the impurity concentration, and ε_0 and ε_r are the vacuum and relative permittivities, respectively. When $f_E \approx f_p$, a feedback process of the OPPTR phenomenon takes place by means of the electric field fluctuations so that relevant current oscillations of frequency f_E are possible.[7,13]

Additionally, for the feedback action of the electric field to be effective, a minimum distance between electron accumulations $l_{0\,\mathrm{min}}$ must exist in such a manner that long-range Coulomb interaction between adjacent carrier accumulations can be strong enough. The value of $l_{0\,\mathrm{min}}$ should be related to the Debye length of the material

$$\lambda_D = \sqrt{\frac{K_B T \varepsilon_0 \varepsilon_r}{Ne^2}}, \tag{5}$$

with K_B being the Boltzmann constant and T the temperature. As will be observed in the results of the simulations, $l_{0\,\mathrm{min}}$ must be several times longer than λ_D for the oscillations to appear.

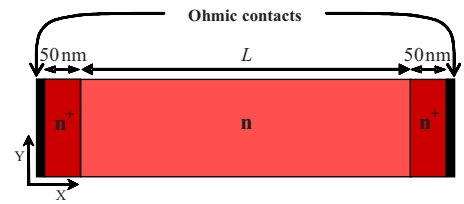

FIG. 1. (Color online) Scheme of the simulated GaN n^+nn^+ diodes.

Finally, it is also necessary that electrons start the process with a very low velocity dispersion, a condition that can be achieved in n^+nn^+ diodes where the doping levels of the n^+ and n regions are sufficiently different because of the high potential barrier that electrons find when they are injected into the n region. More details about the conditions under which the OPPTR phenomenon takes place and the onset of related oscillations in a device can be found in Refs. 7 and 20.

III. MC MODEL AND SIMULATED STRUCTURES

We have analyzed the OPTTR in GaN n^+nn^+ diodes by means of an ensemble MC simulator self-consistently coupled with a two-dimensional Poisson solver. The conduction band of GaN is modeled by three nonparabolic spherical valleys (Γ_1, U and Γ_3) and the considered scattering mechanisms are acoustic, optical, and intervalley phonons, ionized impurities, dislocations, and piezoelectric scattering. It is important to underline that since these diodes are vertical structures, dislocations are essentially parallel to the electron transport, and therefore this scattering mechanism has a negligible influence on the results.

The simulated GaN n^+nn^+ diodes (see Fig. 1) have a low doped n region of length L between two 50 nm n^+ layers, with a doping two orders of magnitude higher than that of the n region. Ohmic contacts are considered in the n^+ regions at the boundaries of the diodes.[25] L and n will be varied in the calculations to identify their influence on the results.

In order to easily perform a frequency analysis of electrical fluctuations and to detect the presence of current oscillations, the time-domain current sequences obtained from the MC simulations are Fourier transformed (once subtracted the average value) into the frequency domain to determine the current noise spectra.

IV. RESULTS

Using a single particle simulator, we have initially analyzed the conditions under which the electron dynamics is dominated by the OPPTR. To this end, velocity sequences of a single electron traveling in bulk GaN under the action of a constant electric field have been calculated at different temperatures, as shown in Fig. 2, for an electric field of 2 kV/cm.

At very low temperature, 15 K [Fig. 2(a)], the velocity sequence exhibits a periodic behavior quite similar to what was explained before for the OPPTR dynamics: accelerations and subsequent stops when emitting the optical phonons. The

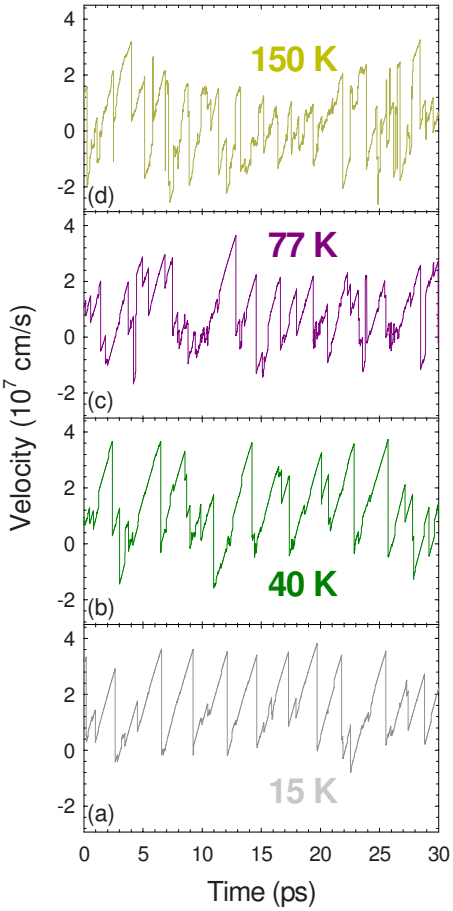

FIG. 2. (Color online) Sequences of instantaneous velocity of a single electron under the action of an electric field of 2 kV/cm at different temperatures in GaN (doped 10^{15} cm^{-3}).

period of the velocity oscillations observed in the sequence is slightly longer than the theoretical one, given by Eq. (2). This is due to the influence of other scattering mechanisms that also take place at low temperature (acoustic phonons, ionized impurities, and piezoelectric scattering), recognized in the plot as small instantaneous reductions in velocity. However, due to the essentially elastic and anisotropic (small velocity deviation) character of these collisions, their influence is practically negligible and it is OPE which dominates carrier dynamics. As temperature increases [Figs. 2(b)–2(d)], other scattering mechanisms compete more and more with OPE, especially with the onset of optical phonon absorption, and thus the electron motion progressively loses its periodic behavior (practically undetectable beyond 40 K). The mechanism of absorption of optical phonons can be clearly identified by abrupt increases in velocity, already present at 77 K and quite frequent at 150 K.

Figure 3 shows the *I-V* curve of a GaN n^+nn^+ diode with an n region with length of $L=2$ μm and doping of 10^{15} cm^{-3} calculated at 15 K. When the applied voltage reaches the threshold for one OPE, which is $\hbar\omega_0/e=0.091$ V, and also at twice and three times such a value, the curve shows unusual humps, as found experimentally in diodes made of other materials.[15–18] Moreover, as observed in the current sequences of the inset, the current exhibits an oscillatory behavior in the bias range from 0.1 to 0.5 V approximately.

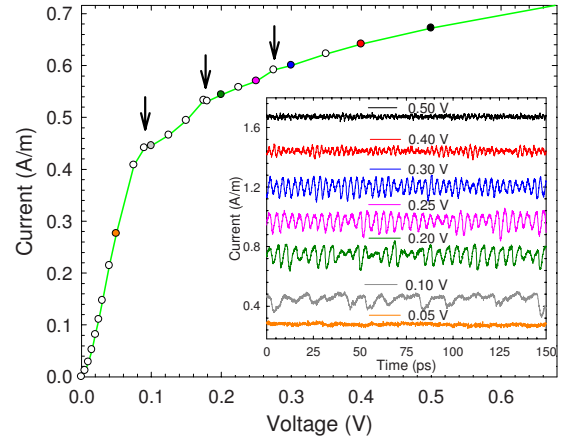

FIG. 3. (Color online) *I-V* curve, calculated at 15 K, of a GaN n^+nn^+ diode with a doping/length of the n^+ and n regions of 10^{17} cm^{-3}/50 nm and 10^{15} cm^{-3}/2 μm, respectively. The arrows indicate the bias points at which electrons reach the energy to undergo one, two, and three OPEs while crossing the n region. The inset shows the time evolution of the current for different voltages. In order to improve the readability, the curves are vertically shifted by 0.2 A/m each, starting from the one corresponding to $V=0.2$ V.

To understand the phenomenon, profiles of OPE rate and electric field along the diode for different applied voltages are shown in Fig. 4. As observed, due to the localized injection of low-energy carriers in the n active region at the source n^+n interface, the emissions take place also at some localized, spatially periodic, regions [Fig. 4(a)], where carriers stop. The associated electron accumulations at these stopping regions give rise to the so-called spatial free carrier grating,[13] with the consequent inhomogeneity of the electric field profile [Fig. 4(b)]. An increasing number of (closer)

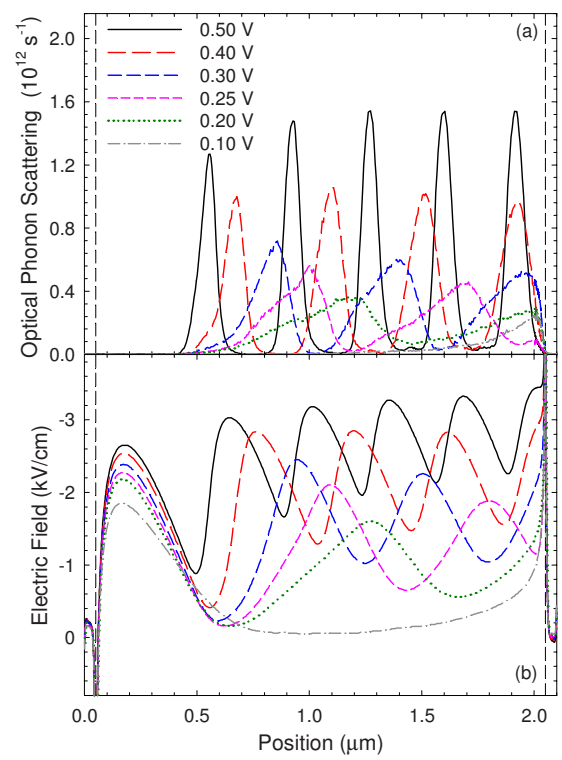

FIG. 4. (Color online) Profiles of (a) OPE rate and (b) electric field along the diode of Fig. 3 at 15 K for different voltages.

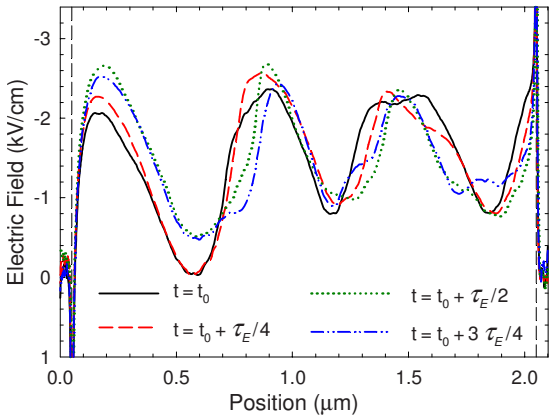

FIG. 5. (Color online) Profile of the electric field for several equidistant times within one period of oscillation for an applied voltage of $V=0.3$ V in the diode of Fig. 3. The temperature is 15 K.

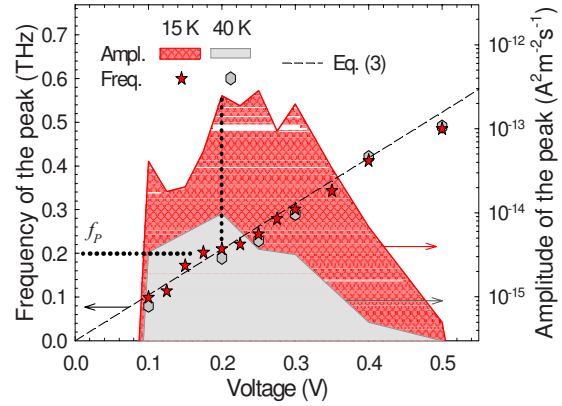

FIG. 6. (Color online) Frequency of the oscillations and amplitude of the corresponding peak in the spectral density (left and right axes, respectively) as a function of the applied voltage in the diode of Fig. 3 at 15 and 40 K. The theoretical oscillation frequency given by Eq. (3) is also plotted.

emission zones is observed as the applied voltage increases, the distance l_0 between them following Eq. (1) correctly.

At first sight, it may seem that there are no significant qualitative differences between the curves in Fig. 4(a): all of them show the expected spatially periodic behavior, the number of stop zones being equal to the integer part of the ratio $eV/\hbar\omega_0$. However, actually, there is a very significant difference: while for low voltages the emission regions are more spread out, as the voltage increases, the profiles show a more defined shape, with a clear localization of the emission regions. This feature is key for determining the presence or absence of current oscillations.

As explained in Sec. II, to have current oscillations in the diode, it is necessary to synchronize in time the OPEs taking place at different positions in the active region, which is only possible through the feedback provided by the self-consistent electric field. Figure 5 shows the electric field profile at several equidistant times within one period of oscillation for the case of $V=0.3$ V. When an OPE occurs at a given position, a local increase in the electron concentration takes place, which couples to the electric field, leading further OPEs to be delayed in time and shifted in space, thus originating the observed current oscillations. To provide this synchronizing feedback, the profile of the electric field evolves in time during the period of the oscillation, as observed in Fig. 5, and it causes the spread-out shape of the time-average profiles of Fig. 4(a) in the case of applied voltages for which clear oscillations are observed in the current. As the applied voltage increases, the separation between accumulation regions l_0 decreases, becoming shorter than the minimum distance $l_{0\,\mathrm{min}}$ necessary to have a feedback of the electric field strong enough to synchronize the OPEs taking place at different positions. For instance, in the case shown in Fig. 4, when l_0 becomes shorter than about 20 times the Debye length corresponding to the doping of the n region, the current oscillations practically disappear (that happens for $V>0.4$ V, see Fig. 3). In such cases, there is no time evolution of the electric field profile and clearly localized emission zones are observed in Fig. 4.

The spectral analysis of the current sequences obtained from MC simulations evidences the presence of a clear peak in the spectral density of current fluctuations at the fundamental frequency of the oscillations and also lower peaks at its first harmonics. The dependence of the fundamental frequency on the applied bias, shown in Fig. 6, follows closely the theoretical estimation provided by Eq. (3), with $E=V/L$. Regarding the amplitude of the oscillations, its maximum value is achieved around the plasma frequency of the n region, 0.2 THz in this case, which confirms the important role played by plasma oscillations in the feedback process by the electric field.

When the temperature is increased to 40 K, current oscillations are much weaker than for 15 K and the bias range with significant current oscillations extends only up to 0.3 V (Fig. 6). This is due to two reasons. On the one hand, by increasing temperature, other scattering mechanisms become more probable and compete with OPE [see Fig. 2(c)], the coherence of the phenomenon being degraded. Also, on the other hand, the Debye length increases with temperature so that the range of voltages for which l_0 is longer than $l_{0\,\mathrm{min}}$ (approximately 20 times the value of the Debye length) is shorter. The frequency of the oscillations f_E coincides with the case of lower temperature, following the theoretical value given by Eq. (3), independent of temperature. If the temperature is further increased to 77 K, the OPTTR practically disappears and no current oscillation is observed, whereas the free carrier grating becomes fuzzier.

By varying the length of the n region L (keeping $T=15$ K), the results shown in Figs. 7 and 8 are obtained. When L is reduced to 1 μm (Fig. 7), oscillations take place only up to around 0.225 V, which means a maximum of two OPEs along the n region [Fig. 8(a)]. The amplitudes of the peaks in the spectral density are much smaller than for $L=2$ μm and the frequencies are somewhat below the theoretical prediction. If L is further reduced to 0.5 μm, current oscillations do not appear at all. For $L=3$ μm, current oscillations are present in a much wider bias range (0.1–0.6 V), giving place to more stop zones along the n region [Fig. 8(b)]. Additionally, the frequency versus bias curve (Fig. 7) shows a good agreement with the behavior predicted by Eq. (3) and the amplitude of the peaks is similar to the case of $L=2$ μm. Note that by increasing L, the frequency of

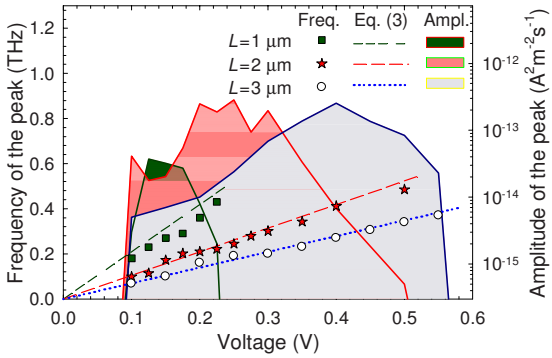

FIG. 7. (Color online) Frequency of the oscillations and amplitude of the corresponding peak in the spectral density as a function of the applied voltage for different lengths of the n region (doped 10^{15} cm^{-3}) at 15 K. The theoretical oscillation frequencies for each case are also plotted.

the oscillations taking place for a given applied voltage is lower since it scales with the value of the electric field (inversely proportional to L). Again, for all the values of L, the maximum amplitude of the oscillations corresponds to frequencies close to that of the plasma.

From the last results, it can be concluded that by varying the length of the n region, the voltage range where current oscillations are present is modified, and also the amplitude of the peaks may change, but the maximum attained frequency is similar in all cases. To increase the frequency range of the oscillations induced by the OPTTR, the most straightforward possibility is to use n^+nn^+ structures with larger doping,

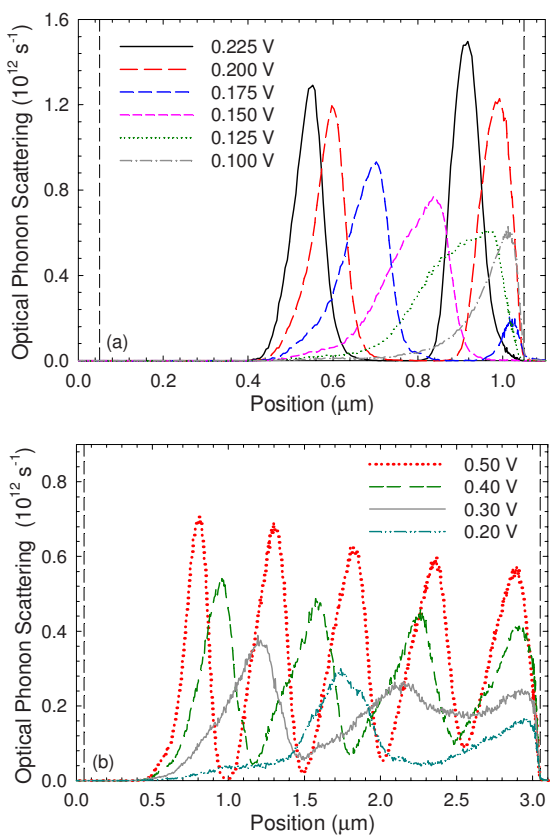

FIG. 8. (Color online) Profile of the OPE rate at 15 K for different lengths of the n region (doped 10^{15} cm^{-3}) at 15 K: (a) $L=1$ μm and (b) $L=3$ μm.

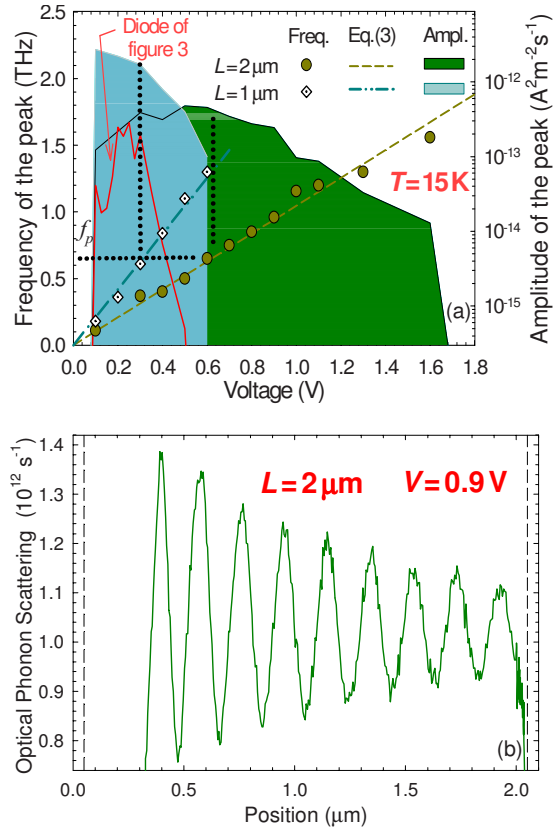

FIG. 9. (Color online) (a) Frequency of the oscillations and amplitude of the corresponding peak in the spectral density as a function of the applied voltage for two diodes with high doping ($n^+=10^{18}$ cm^{-3} and $n=10^{16}$ cm^{-3}) and different lengths ($L=1$ and 2 μm) at 15 K. In order to compare the results, the amplitude of the peak in the diode of Fig. 3 ($L=2$ μm) is also plotted. (b) Profile of the OPE rate in the diode with $L=2$ μm for $V=0.9$ V.

where oscillations are expected to be sustained up to higher frequencies because of the increased plasma frequency.

Figure 9(a) presents the results (at 15 K) for diodes with a doping one order of magnitude higher than in the previous structures both in the n and n^+ regions (10^{16} and 10^{18} cm^{-3}, respectively) and two different lengths ($L=1$ μm and $L=2$ μm). Space charge effects are obviously enhanced by the higher doping, thus providing oscillations with larger amplitude, especially in the shorter diode. Moreover, these oscillations persist up to higher voltages as compared to the corresponding results with the same length and lower doping. This is due to the smaller value of the Debye length at increasing doping [Eq. (5)] and the shorter associated $l_{0\,\mathrm{min}}$. Now, the plasma frequency of the n region is 0.64 THz and this allows obtaining significant current oscillations with frequencies above 1 THz, which constitutes the most remarkable result of this work.

Figure 9(b) shows the profile of OPE rate for $V=0.9$ V in the diode with $L=2$ μm. Nine stop zones are clearly visible. As observed, the amplitude of the modulation decays along the n region [also happening in Fig. 8(b) for a high number of stop regions]. This is probably the reason why the amplitudes of the peaks for $L=2$ μm shown in Fig. 9(a) are not as high as for $L=1$ μm. When L increases, it is not possible to get a perfect synchronization of such a high num-

ber of OPEs along the n region since the probability of having scattering mechanisms other than OPEs increases.

V. CONCLUSIONS

With the help of a MC simulator, current oscillations induced by OPTTR in GaN n^+nn^+ diodes at low temperature have been analyzed. OPTTR originates charge accumulations along the n region of the diodes in the zones where OPEs take place, which tend to oscillate at its plasma frequency f_P. When f_P is close to the inverse of the time interval between OPEs, f_E, and charge accumulations are separated enough from each other (to guarantee the synchronization of the OPEs along the diode through the feedback provided by the self-consistent electric field), important current oscillations of frequency f_E appear. The profiles of various magnitudes such as OPE rate or electric field show the associated inhomogeneities in time and space.

Obviously, when temperature is raised, the coherence is degraded mainly because of the growing influence of other scattering mechanisms. By increasing the length of the n region, current oscillations take place in a wider bias range, but without any improvement in the maximum frequency of oscillation. A frequency enhancement can be achieved by increasing the doping of the diode; for $n=10^{16}$ cm^{-3} and $n^+=10^{18}$ cm^{-3}, current oscillations with frequencies above 1 THz are obtained in the 1–2 μm diodes.

ACKNOWLEDGMENTS

This work has been partially supported by the Dirección General de Investigación (MEC) and FEDER (Project No. TEC2007-61259/MIC and Acción Integrada Project No. HF2007-0014) and by the Consejería de Educación, Junta de Castilla y León (Project Nos. SA019A08 and GR270).

[1] *Terahertz Spectroscopy: Principles and Applications*, edited by S. Dexheimer (CRC, Boca Raton, FL, 2007).
[2] M. C. Beard, G. M. Turner, and C. A. Schmuttenmaer, Phys. Med. Biol. **47**, 3841 (2002).
[3] P. H. Siegel, IEEE MTT-S Int. Microwave Symp. Dig. **3**, 1575 (2004).
[4] Y. S. Lee, *Principles of Terahertz Science and Technology* (Springer, New York, 2008).
[5] J. Faist, F. Capasso, D. L. Sivco, C. Sirtori, A. L. Hutchinson, and A. Y. Cho, Science **264**, 553 (1994).
[6] L. Varani, C. Palermo, J. F. Millithaler, J. C. Vaissière, E. Starikov, P. Shiktorov, V. Gružinskis, J. Mateos, S. Pérez, D. Pardo, and T. González, J. Comput. Electron. **5**, 71 (2006).
[7] E. Starikov, P. Shiktorov, V. Gružinskis, L. Varani, C. Palermo, J. F. Millithaler, and L. Reggiani, J. Phys.: Condens. Matter **20**, 384209 (2008).
[8] B. Foutz, S. O'Leary, M. S. Shur, and L. F. Eastman, J. Appl. Phys. **85**, 7727 (1999).
[9] K. Brennan and K. Hess, Solid-State Electron. **27**, 347 (1984).
[10] V. Gružinskis, E. Starikov, and P. Shiktorov, J. Comput. Electron. **6**, 11 (2007).
[11] V. Gružinskis, P. Shiktorov, and E. Starikov, Acta Phys. Pol. A **113**, 947 (2008).
[12] E. Starikov, P. Shiktorov, V. Gružinskis, L. Reggiani, L. Varani, and J. C. Vaissière, J. Comput. Electron. **2**, 465 (2003).
[13] V. Gružinskis, P. Shiktorov, E. Starikov, L. Reggiani, L. Varani, and J. C. Vaissière, Semicond. Sci. Technol. **19**, S173 (2004).
[14] V. Gružinskis, E. Starikov, and P. Shiktorov, Acta Phys. Pol. A **107**, 163 (2005).
[15] Y. Katayama and K. F. Komatsubara, Phys. Rev. Lett. **19**, 1421 (1967).
[16] T. W. Hickmott, P. M. Solomon, F. F. Fang, F. Stern, R. Fischer, and H. Morkoç, Phys. Rev. Lett. **52**, 2053 (1984).
[17] P. F. Lu, D. C. Tsui, and H. M. Cox, Phys. Rev. Lett. **54**, 1563 (1985).
[18] P. F. Lu, D. C. Tsui, and H. M. Cox, Phys. Rev. B **35**, 9659 (1987).
[19] L. E. Vorob'ev, S. N. Danilov, V. N. Tulupenko, and D. A. Firsov, JETP Lett. **73**, 219 (2001).
[20] E. Starikov, P. Shiktorov, V. Gružinskis, L. Varani, C. Palermo, G. Sabatini, H. Marinchio, T. Laurent, and L. Reggiani, J. Stat. Mech.: Theory Exp. 2009, P01035.
[21] V. Gružinskis, P. Shiktorov, and E. Starikov, Acta Phys. Pol. A **113**, 943 (2008).
[22] P. Shiktorov, V. Gružinskis, E. Starikov, L. Reggiani, and L. Varani, Semicond. Sci. Technol. **12**, 1331 (1997).
[23] E. Starikov, P. Shiktorov, V. Gruzinskis, L. Reggiani, L. Varani, J. C. Vaissiere, and J. H. Zhao, IEEE Trans. Electron Devices **48**, 438 (2001).
[24] R. O. Dendy, *Plasma Dynamics* (Oxford University Press, New York, 1990).
[25] T. González and D. Pardo, Solid-State Electron. **39**, 555 (1996).